JOURNAL OF CATALYSIS, 95, 209–219 (1985)

Role of Iron in Multicomponent Molybdate Catalysts for Selective Oxidation of Propylene[1]

T. S. R. PRASADA RAO AND K. R. KRISHNAMURTHY

Research Centre, Indian Petrochemicals Corporation Limited, Baroda-391 346, India

Received April 25, 1984; revised April 2, 1985

In order to investigate the role of iron in multicomponent molybdate (MCM) catalysts, a series of MCM catalysts of the composition $Mg_{11-x}Fe_xBiMo_{12}O_n$ ($0 \le x \le 8$) have been prepared and characterized by X-ray diffraction, infrared, thermal analysis, Mössbauer spectroscopy, scanning electron microscopy, and electron spectroscopy for chemical analysis (ESCA). In samples with a value of x up to 2.0, the formation of a ternary compound, $Bi_3(FeO_4)(MoO_4)_2$ is observed. At $x = 2.5$ the ternary compound and ferric molybdate coexist and on increasing the value of x, ferric molybdate is formed. At $x = 8$, ferric molybdate exists as a major phase with β-$MgMoO_4$, $Bi_2(MoO_4)_3$ and small amounts of α-Fe_2O_3. ESCA data have shown that the surface concentrations of Bi and Mo increase with increasing addition of Fe, though their bulk composition remains unaltered throughout the series. The highest Bi/Mo ratio is observed at $x = 2.5$. Activity and selectivity for oxidation of propylene at 430°C over the series of catalysts also increase with the value of x, exhibiting maxima again at $x = 2.5$. An attempt has been made to rationalize the observed activity pattern on the basis of the physiochemical characteristics. Formation of ternary compound and enrichment of the surface with key components, i.e., Bi (for rate-determining α-H abstraction step) and Mo (for selective oxygen insertion) are responsible for the enhancement observed up to $x = 2.5$. Maximum surface Bi/Mo ratio corresponds to maximum activity and selectivity. At higher values of x, absence of ternary compound and formation of higher amounts of $Fe_2(MoO_4)_3$ and some free α-Fe_2O_3 results in poor performance.

INTRODUCTION

A major breakthrough in the development of catalysts for oxidation/ammoxidation of olefins was the discovery of the promoting action of iron in bismuth phosphomolybdate catalysts (*1*). Although a number of other elements like Ni, Co, Cr, Mn, and K were later introduced to form the most efficient multicomponent molybdate (MCM) catalysts (*2*), iron continued to be an important constituent in both molybdenum (*3*) and antimony (*4*)-based catalysts. As iron was recognized to be the most efficient promotor element in molybdate catalysts, a number of investigations were undertaken to study the role of iron and a review of Keulks *et al.* (*5*) gives an account of such studies. Earlier studies by Annenkova *et al.* (*6*) revealed that Bi–Mo–Fe ternary system consisted of $Bi_2(MoO_4)_3$, $Fe_2(MoO_4)_3$, Bi FeO_3, and $Bi_2Fe_4O_9$. Batist and co-workers (*7*) reported the formation of compound "X" in the ternary system. A systematic study on the formation, physicochemical characterisation, and the activity of ternary compounds involving Bi–Fe–Mo was later reported by Keulks *et al.* (*8–10*), and Sleight *et al.* (*11, 13*). These studies provided ample evidence for the formation of a well-defined ternary compound, $Bi_3(FeO_4)(MoO_4)_2$ in Bi–Fe–Mo system, which enhances its activity and selectivity for the partial oxidation of olefins. However, the role of iron in more complex MCM catalyst systems like $Mo_aFe_bBi_cMe_bP_iK_gO_n$ (where *Me* = Ni, Co, or Mg) is yet to be understood clearly. Wolfs and Matsura (*14*) in their studies on the system $Mg_{11-x}Fe_xMo_{12}BiO_n$ ($0 \le x \le 4$) concluded that maximum activity and selectivity is displayed when $x = 2.5$ but could not explain the significance of optimum iron concentration. Van Oeffelen (*15*) pursued stud-

IPCL Communication No. 79.

0021-9517/85 $3.00

ies in the same system and arrived at the conclusion that the role of iron is to maintain Bi in oxidized state, by functioning as a redox couple and to account for the optimum iron level at $x = 2.5$ an equation of $Bi^0 + 3Fe^{3+} \rightarrow Bi^{3+} + 3Fe^{2+}$ was proposed. The role of iron as redox couple was again brought out by Batist (*16*). Our earlier work (*17*) on fresh and used silica-supported MCM catalysts for ammoxidation of propylene indicated the presence of iron as $Fe_2(MoO_4)_3$ in fresh catalyst and its reduction to $FeMoO_4$ during use. Apart from functioning as redox couple, iron could also be involved in the formation of ternary compounds which can display better activity and selectivity (as in the case of simple bismuth molybdate). Such a possibility was not ruled out by earlier workers (*5, 15*). Recently Forzatti *et al.* (*18*) observed the formation of the compound $Bi_3(FeO_4)(MoO_4)_2$ in the case of ferric molybdate doped with varying amounts of bismuth. In order to clarify the above points and to probe into the reasons for the optimum concentration of iron ($x = 2.5$) in MCM catalysts detailed investigations have been carried out in our laboratory on the system $Mg_{11-x}Fe_xBiMo_{12}O_n$ with the value of x varying from 0 to 8. The results on physiochemcical characterization of the catalysts, activity measurements, and their interrelationship are described.

EXPERIMENTAL METHODS

Preparation of the catalysts. The catalyst samples were prepared by slurry method adopted by Wolfs and Batist (*19*). Required amounts of Fe, Bi, and Mg as their respective nitrates were dissolved in 200 ml of water with 5 ml of concd HNO_3 and heated up to 70°C with constant mechanical stirring. Appropriate quantity of Mo as MoO_3 powder was added to the hot solution, with vigorous mixing and using dilute ammonia pH was adjusted to 5. The solution containing a brown precipitate was then heated to form a slurry, which was dried at 110°C for 16 h, precalcined at 320°C for 2 h and finally calcined at 520°C for 8 h to obtain the catalyst. All the reagents used were of AnalaR grade. Starting from the parent compound $Mg_{11}BiMo_{12}O_{48.5}$, 12 samples, with varying amounts of iron were prepared. Chemical composition of the prepared samples were determined by wet analysis using atomic absorption spectroscopy and were found to be as expected. Details of sample composition code number and BET surface area values are given in Table 1.

Characterization of the catalysts. The X-ray diffractograms of the samples were recorded with Phillips PW 1130 generator, with Ni-filtered CuKα ($\lambda = 1.5418$ Å) radiation, and a proportional counter. IR spectra were recorded using Beckman Model 4220 double-beam spectrometer by KBr-disk technique. The thermograms were obtained with MOM derivatograph at a heating rate of 10°C/min. Scanning electron microphotographs were prepared from Jeol Model J35C scanning electron microscope. Electron spectroscopy for chemical analysis (ESCA) spectra were recorded using VG Model ESCA Mark II at 15 kV and 20 mA with AlKα line (1486.6 kV). The binding energy values were corrected with respect

TABLE 1

Composition and Surface Area of the System $Mg_{11-x}Fe_xBiMo_{12}O_n$

Sr. No.	Code No.	Iron content (x)	Surface area (m^2/g)	Phases identified[a]
1	FE0	0.00	5	A, B, C, D
2	FE1	0.25	2	B, C, E
3	FE2	0.50	6	B, C, E
4	FE3	0.75	4	B, C, E
5	FE4	1.00	5	B, C, E
6	FE5	1.50	9	B, C, E
7	FE6	2.00	3	B, C, E
8	FE7	2.50	4	B, F, C, E
9	FE8	3.00	5	B, F, C
10	FE9	4.00	5	B, F, C
11	FE10	6.00	6	B, F, C, D
12	FE11	8.00	6	B, F, C, D

[a] A, α-$MgMoO_4$; B, β-$MgMoO_4$; C, $Bi_2(MoO_4)_3$; D, Bi_2MoO_6; E, $Bi_3(FeO_4)(MoO_4)_2$; F, $Fe_2(MoO_4)_3$.

to C_{1s} line positioned at 285 eV. The atomic ratios were computed from the intensity of the photoelectron peaks by adopting the method proposed by Carter *et al.* (*20*). Photoelectron cross section values reported by Scofield (*21*) were used. The Mössbauer spectra were recorded at 298 K using 5 mCu^{57}Co source embedded in Rh matrix. Isomer shift values were measured with respect to the center of hyperfine pattern of pure α-Fe_2O_3 and corrected w.r.t. α-Fe. BET surface area values (variable within ±10%) were obtained by adsorption of nitrogen at liquid-nitrogen temperature.

Evaluation of activity and selectivity. Activity measurements were carried out under steady-state flow conditions using a stainless-steel tube reactor (length 30 cm, diam. 20 mm) filled with 1 g of catalyst (+90 to −250 μm in size). The particle sizes were so chosen to eliminate external and internal diffusion limitations. The catalyst bed was kept fixed with the help of Pyrex glass-wool plugs on either side, followed by glass beads. The reactor temperature was monitored by two thermocouples, one inside the thermowell located at the center of the catalyst bed and the other attached to the outer wall of the reactor. The temperature of the outer thermocouple was controlled so that the inner thermocouple indicated the desired bed temperature. Initially, the catalyst bed was heated to 420°C in a stream of pure and dry nitrogen. At 420°C, air (70 ml/min) was introduced in place of nitrogen followed by propylene (10 ml/min). An increase in bed temperature (~10°C) was noticed. The bed temperature was set at 430°C, by adjusting the outer thermocouple temperature thereafter, the bed temperature was maintained within ±2°C. The reactor attained steady state within 1 h as indicated by constant conversions of propylene with time. The empty reactor (with glass wool and glass beads packing) did not show any measurable activity under identical conditions. The reaction products were analyzed by an "online" gas chromatograph, connected to the reactor outlet through a gas-sampling valve.

From the analysis of reactants and products (propylene, air, acrolein, CO, CO_2, and H_2O), the conversion of propylene and selectivity for acrolein formation were calculated as follows

$$\% \text{ Conversion} = \frac{\text{Moles of propylene reacted}}{\text{Moles of propylene fed}} \times 100$$

$$\% \text{ Selectivity} = \frac{\text{Moles of acrolein formed}}{\text{Moles of propylene reacted}} \times 100$$

Conversion and selectivity values were reproducible within ±2% error. The degree of reduction of the catalyst during reaction, expressed as reduction number, was determined by dissolving the catalyst in H_2SO_4 and titrating with $KMnO_4$.

RESULTS AND DISCUSSION

1. Physiochemical Characterization

1.1 X-Ray diffraction studies. It is observed that the parent compound FE0 (with no iron) is a mixture of α- and β-$MgMoO_4$ (3.34 and 3.39 Å) (*15*), α-bismuth molybdate (3.198 and 3.068 Å), and γ-bismuth molybdate (3.15 Å). The introduction of the very first dose of iron (x = 0.25) transforms all α-$MgMoO_4$ to β-$MgMoO_4$, as shown by the disappearance of the characteristic "*d*" lines of the α-phase (3.34, 3.67, and 3.86 Å). Such a stabilization of β-phase by iron has been observed earlier by Wolfs (*19*) and Van Oeffelen (*15*) and is attributed to the formation of ferric molybdate, $Fe_2(MoO_4)_3$ (abbreviated FM). However, in the present investigation, no "*d*" lines corresponding to FM could be observed in samples up to x = 2. From the sample FE7 (x = 2.5) onward, characteristic "*d*" lines due to FM start appearing in the XRD (X-ray diffraction) patterns. As the concentration of iron increases, the lines due to FM increase in intensity and for FE11 (x = 8) sample, FM appears as the

major phase. This observation indicates that at low iron concentration, iron could be involved in a ternary compound formation and at higher concentrations it appears as FM. XRD patterns of such ternary compounds, $Bi_3(FeO_4)(MoO_4)_2$ have been reported earlier by Keulks *et al.* (*10*) and Sleight *et al.* (*11*). The ternary compound is characterized by two doublets, 3.17 and 3.15 Å and 4.88 and 4.78 Å. Of the two, the doublet at 3.17 and 3.15 Å is present in all the compounds including FE0 and hence could not be taken as evidence for the formation of ternary compounds in the system, Mg_{11-x} $Fe_xBiMo_{12}O_n$. However, the other doublet (4.88 and 4.78 Å), and another line at 2.91 Å, which are also characteristic of the ternary compound, are observed in the XRD patterns of the samples FE1 to FE7. Significantly these lines do not appear in the XRD patterns of the samples FE8 to FE11, thereby indicating that the ternary compound is formed up to FE7, after which added iron goes to form FM. The results of XRD studies summarizing the phases identified in different samples are given in Table 1.

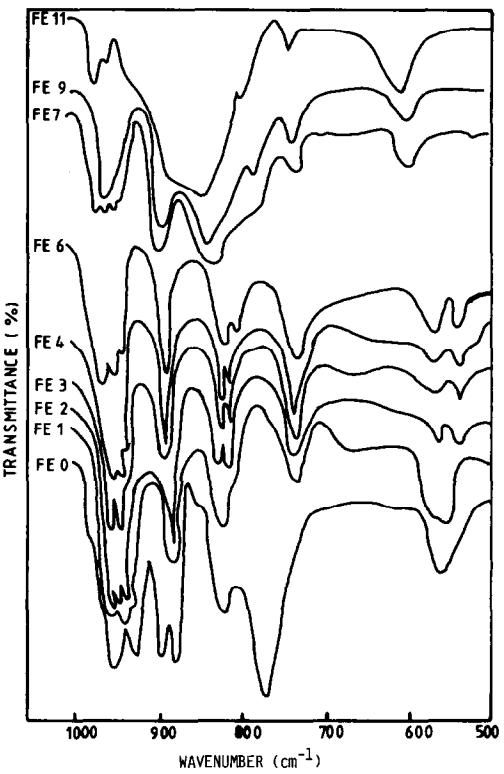

FIG. 1. Infrared spectra of the catalysts.

1.2 IR spectroscopic studies. Infrared spectra of the samples are presented in Fig. 1. The parent compound FE0 reveals all the characteristic absorption bands of $MgMoO_4$ (*22*) and α- and γ-bismuth molybdates (*23*). With the addition of iron (at x = 0.25) the strong band at 775 cm^{-1} is shifted to 745 cm^{-1}. On the basis of XRD evidence, the above shift could be attributed to the transformation of α-$MgMoO_4$ to β-form. With increasing iron concentration, additional absorption bands appear at 885, 815, 565, and 530 cm^{-1}. The band at 825 for FE0 is shifted to 840 cm^{-1}. Keulks *et al.* (*9*) identified IR absorption bands at 880, 845, 815, 750, 575, and 540 cm^{-1} for the ternary compound $Bi_3(FeO_4)(MoO_4)_2$. The presence of these bands in the IR spectra of samples FE1 to FE7 shows that ternary compound is formed in these samples. However, major changes are observed again with FE7 wherein the band at 840 cm^{-1} is shifted toward 830 cm^{-1} (characteristic of FM), the band at 815 cm^{-1} is almost absent and the doublet 565 and 530 cm^{-1} merge to form a single band at 550 cm^{-1}. From FE8 onward the band at 830 cm^{-1} increases in intensity (with broad diffused shape) at the expense of the bands at 885 and 730 cm^{-1} (due to $MgMoO_4$) and a new band develops at 600 cm^{-1}. The growth of the band at 830 cm^{-1} indicates the increase in the concentration of FM, and the disappearance of bands at 815, 565, and 530 m^{-1} points out the decomposition of the ternary compound, possibly with the formation of α-Fe_2O_3, with a characteristic band at 600 cm^{-1}. All these observations indicate that the ternary compound $Bi_3(FeO_4)(MoO_4)_2$ is formed in samples up to x = 2.5, wherein iron molybdate also coexists and from FE8 onward iron molybdate phase predominates.

1.3 Thermogravimetric studies. The ther-

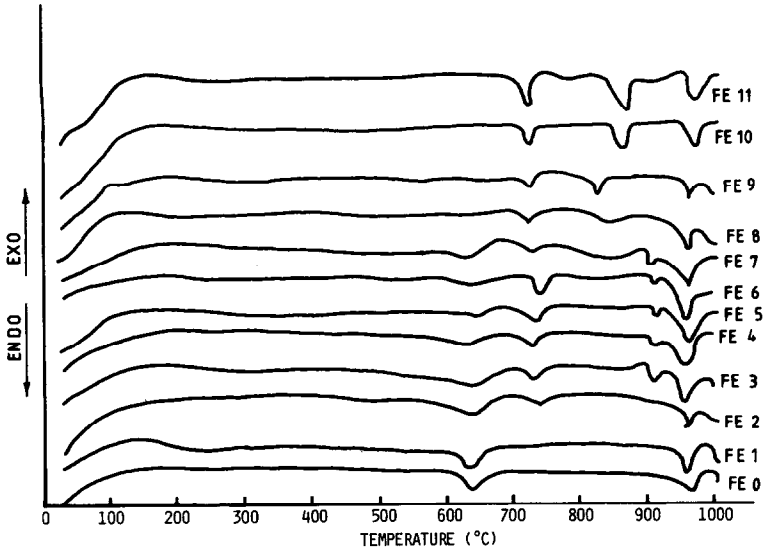

FIG. 2. Thermograms of the catalysts.

mograms of the samples are given in Fig. 2. The DTA curve for the parent compound (FE0) shows two endothermic peaks, one around 640°C due to fusion of $Bi_2(MoO_4)_3$ (*24*) and the other around 960°C due to $MgMoO_4$ and Bi_2MoO_6. With the addition of iron, an additional endothermic peak appears in the range 900–915°C, which is close to the melting point of ternary compound reported by Keulks *et al.* (*9*) (908–912°C) and Sleight *et al.* (*12*) (925°C). The additional peak appears only for the samples FE1 to FE7 and is absent in samples from FE8 onward, indicating that the ternary compound is not formed beyond FE7. Peaks around 620, 720–730°C, are due to phase transformations in Bi_2MoO_6 (*5*) and those at 820 and 860°C may be due to the breakdown of multicomponent molybdate structure, resulting in the formation of some α-Fe_2O_3.

1.4 Mössbauer spectroscopy. Figure 3 presents Mössbauer spectra of a few typical samples in the series. Isomer shift values (w.r.t. α-Fe) and quadrupole splitting values for FE2 are 0.39 ± 0.03 and 0.69 ± 0.03 mm/sec and the corresponding values for FE4 are 0.46 ± 0.03 and 0.86 ± 0.03 mm/sec, respectively. The parameters are comparable with those for Bi–Mo–Fe compounds reported by Keulks *et al.* (*9*) (0.35 ± 0.07 and 1.00 ± 0.07 mm/sec) and Sleight *et al.* (*12*) (0.28 ± 0.01 and 1.04 ± 0.01 mm/sec). Sleight and co-workers have reported

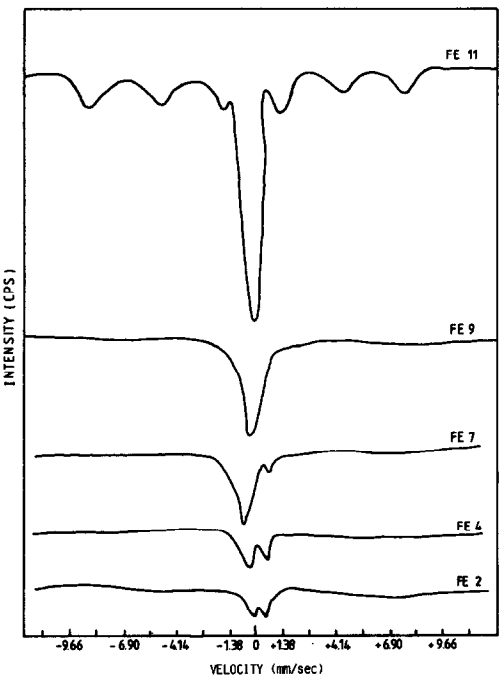

FIG. 3. Mössbauer spectra of the catalysts.

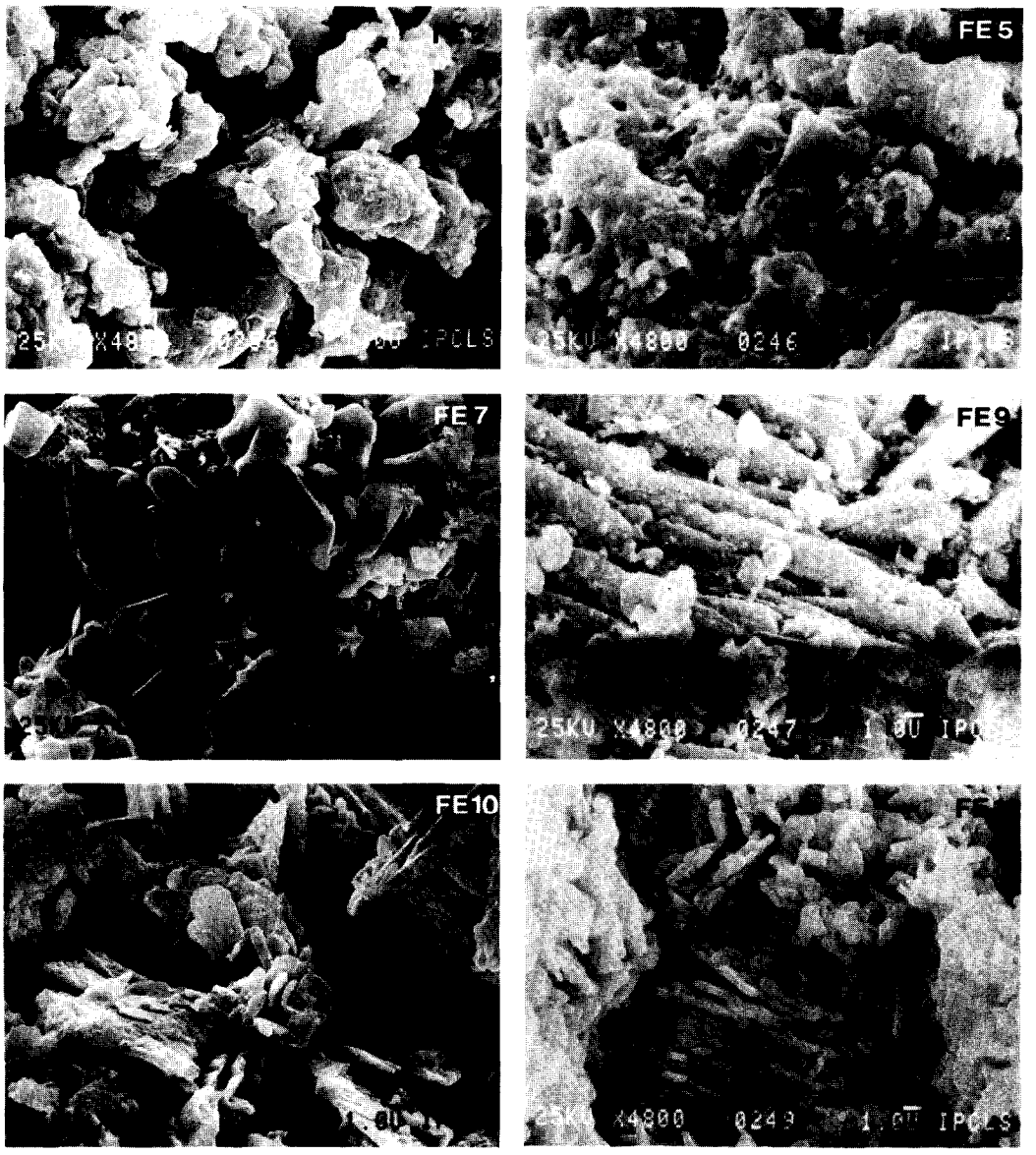

FIG. 4. Segregation of iron molybdate phase as observed by scanning electron microscopy.

parameters for both ordered and disordered $Bi_3(FeO_4)(MoO_4)_2$, but in the present case it is difficult to make such a distinction. Sample FE7 again presents a complex spectrum which consists of a doublet similar to FE2 and FE4, superimposed by a single line due to $Fe_2(MoO_4)_3$. Qualitatively, it can be interpreted that the spectrum reveals the presence of FM as well as ternary compound. Such a complex spectrum (wherein only FM could be identified), for FE7 was observed earlier by Van Oeffelen (*15*). FE9 reveals a clean line due to FM while FE11 shows a sextet attributable to α-Fe_2O_3 along with a single resonance line due to FM. Mössbauer spectroscopy clearly indicates the formation of ternary compound up to $x = 2$, its coexistence with FM at $x = 2.5$ and the formation of α-Fe_2O_3 and FM when $x > 2.5$.

1.5 Scanning electron microscopy. Formation and separation of ferric molybdate phase as revealed by XRD, IR, and derivatographic studies could be further corroborated by electron microscopic studies through the photographs presented in Fig. 4. A careful examination of the crystal habit reveals that all samples up to FE6 appear in distinct plate-like shapes. FE7 shows that appearance of needle-shaped particles, along with plate-shaped ones. Increasing amounts of needle-shaped particles appear in the series FE8 to FE11. A micrograph of FM prepared by the same method also exhibits needle-shaped particles, whose appearance in FE7 marks the separation of FM phase.

1.6 ESCA studies. Figure 5 presents the variation in the surface concentration of Fe, Bi and Mo (expressed as the ratio of M/C intensity, M = Fe, Mo, or Bi), in a few samples in the series. As the concentration of Fe in the bulk increases, a corresponding increase in the surface Fe concentration is observed. However, in the cases of Bi and Mo, the situation appears to be quite different. Throughout the series, the bulk concentration of Bi and Mo are kept constant. As the concentration of added iron increases, the surface gets preferentially enriched with Mo and Bi and a maximum ratio of Bi/Mo is observed for the sample FE7, which also reveals significant variations in XRD in IR data when compared to the samples containing higher or less amount of iron. It is evident that Fe increases the surface concentration of Bi and Mo, when added (up to $x = 2.50$), possibly due to compound formation involving Bi, Fe, and Mo. Thermodynamic conditions (*25*) favor the migration of the ternary compound phase, which has a lower melting point, when compared to $Mg_{11}BiMo_{12}O_n$ or $Fe_2(MoO_4)_3$. As iron concentration is increased further, more and more Fe migrates to the surface, thus disturbing the stable composition range for ternary compound and leading to the formation of iron molybdate. This marks the seggregation of FM phase as indicated by other analytical techniques. With very high Fe concentrations (FE11) some Fe_2O_3 is also formed, as revealed by Mössbauer spectroscopic studies.

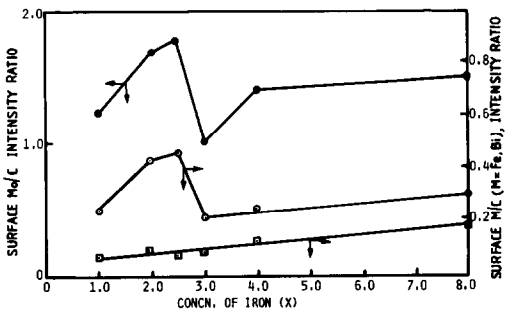

FIG. 5. Variation of surface concentration of Fe, Bi, and Mo with iron content: ●, Mo/C; ⊙, Bi/C; ⊡, Fe/C.

The findings derived from physiochemical characterization studies may be summed up as

(a) Introduction of iron transforms α-$MgMoO_4$ to β-$MgMoO_4$.

(b) At lower iron concentrations (up to $x = 2.0$) a ternary compound, $Bi_3(FeO_4)(MoO_4)_2$ is formed.

(c) At the inflection point (i.e., when $x = 2.5$) the ternary compound coexists with ferric molybdate.

(d) With samples containing more Fe ($x > 2.5$) FM is formed and with FE11 formation of α-Fe_2O_3 is also observed.

(e) Introduction of iron increase the surface concentration of Bi and Mo and the ratio of Bi/Mo in the surface passes through a maximum value at $x = 2.5$.

(f) The state of iron in the samples investigated can be described by the following schemes:

$$Mg_{11-x}Fe_xBiMo_{12}O_n \xrightarrow{x = 0 \text{ to } 2.0}$$

Ternary compound

$$\downarrow x = 2.5$$

Ternary compound + Ferric molybdate

$$\downarrow (2.5 \leq x \leq 8)$$

Ferric molybdate

$$+\alpha\text{-}Fe_2O_3$$

It should be mentioned that Keulks *et al.* (*9, 10*) have proposed another ternary compound with Bi : Mo : Fe ratio of 1 : 1 : 1 and such a compound formation has been observed by Venyaminov and co-workers (*26*) also. As both the ternary phase (1 : 1 : 1 and 3 : 2 : 1) are known to possess identical crystal structure, the presence or absence of 1 : 1 : 1 phase (whose existence has been questioned by Sleight and Linn (*13*)) in the present system could not be established. In view of this any quantitative estimation of the ternary phase could not be attempted. On the basis of the established composition of ternary phase (1 : 1 : 1 or 3 : 2 : 1) it may be expected that some amount of $Fe_2(MoO_4)_3$ exists along with the ternary phase in solid solution even before the stage $x = 2.5$, but no experimental evidence could be obtained in that direction and the seggregation of $Fe_2(MoO_4)_3$ could be observed only at $x = 2.5$.

2. *Relationship between Activity and Physiochemical Characteristics*

The variation in activity and selectivity for the catalysts FE0 to FE11 at a reaction temperature of 430°C is shown in Fig. 6. The activity pattern observed is similar to the one reported earlier by Wolfs and Matsura (*14*). The maximum conversion is displayed by the sample FE7 ($x = 2.5$). Activity for propylene conversion increases along the series FE0 to FE7, while the variation in surface area is irregular, indicating

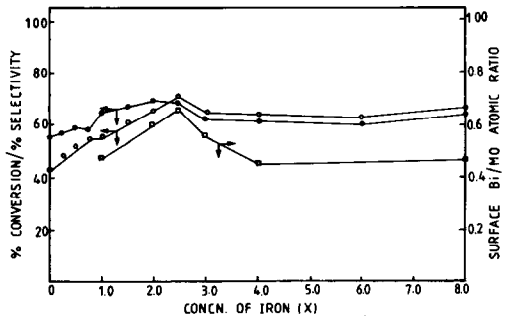

FIG. 6. Variation of conversion (○), selectivity (●), and surface Bi/Mo atomic ratio (□), with iron content.

TABLE 2

Ratio of XRD Line Intensities and Reduction Number Values

Code No.	$I_{(3.15)}/I_{(3.18)}$	Reduction number (meq O_2/g of catalyst)
FE0	0.80	0.041
FE1	0.75	0.043
FE2	1.53	0.170
FE3	1.24	0.140
FE4	0.89	0.250
FE5	0.65	0.340
FE6	0.91	0.580
FE7	0.94	0.560
FE8	0.87	0.670
FE9	0.71	0.89
FE10	0.72	1.13
FE11	0.96	1.54

that the observed activity is not related to surface area.

Earlier studies (*14–16*) on the role of iron in MCM catalysts attributed its promoting action to the improved redox characteristics and stabilization of the active Bi_2MoO_6 phase. However, in the present investigation it is observed that the ratios $I(3.15)/I(3.18)$ which indicate the preferred formation of Bi_2MoO_6 vary irregularly (Table 2) along the series. Hence, it is unlikely that promoting action could be due to the formation of Bi_2MoO_6. As the α-phase, $Bi_2(MoO_4)_3$ also exists along with Bi_2MoO_6 in the parent compound ($Mg_{11}BiMo_{12}O_n$), one would expect that the incorporated iron could form a ternary compound involving Bi, Fe, and Mo, whose structure could be easily derived from that of α-phase. Evidence for the formation of such a ternary compound has been presented in the earlier section on the basis of XRD, IR, Mössbauer, and derivatographic studies.

The formation of ternary compounds is observed in the samples FE0 to FE6 along which activity increases. The sample FE7 consisting of the ternary compound along with ferric molybdate displays maximum activity. Samples FE8 to FE11 which contain ferric molybdate in increasing amounts (and no ternary compound) exhibit decreas-

ing trend in activity. These observations suggest that the increase in activity along the series of samples FE0 to FE7 is due to the formation of ternary compound. ESCA studies on the catalysts, presented earlier, have revealed that introduction of iron induces significant changes in the surface composition. It is observed that the increase in the surface concentration of Bi and Mo (along the series of samples FE0 to FE7), is accompanied by increase in activity. Maximum activity is reached at $x = 2.5$ (sample FE7) where Bi/Mo atomic ratio (0.66) also reaches maximum (Fig. 6). While it is possible that the ternary compound formation on the surface may account for the surface enrichment of Bi and Mo, its relevance to activity/selectivity can be explained on the basis of mechanism of oxidation. In the selective oxidation of propylene (*27*), bismuth ions are responsible for α-hydrogen abstraction step (rate-determining step) and molybdenum–oxygen polyhedra selectively insert oxygen into the π allylic intermediate to give acrolein. In the present case, along the series FE1 to FE7 increase in surface concentration of bismuth contributes toward increase in activity while surface enrichment of molybdenum ensures better selectivity. Apart from the surface Bi/Mo ratio, in a multiphase system like $Mg_{x-11}Fe_xBiMo_{12}O_n$, the interfacial effects between different phases could contribute toward activity. Brazdil and co-workers (*28, 29*) have brought out the importance of such effects in their studies on the model system $Bi_{2-x}Ce_x(MoO_4)_3$. Similarly in the system $Mg_{11-x}Fe_xBiMo_{12}O_n$, the formation of solid solutions involving Bi/Fe/Mo are possible. However, accurate determination of the phases present was difficult, since the phases β-Mg MoO_4, $Bi_2(MoO_4)_3$, $Bi_3(MoO_4)_2(FeO_4)$, and $Fe_2(MoO_4)_3$ contain many diffraction lines which are close in "*d*" values and relative intensity. The separation of $Fe_2(MoO_4)_3$ is observed only when $x = 2.5$. The interfacial regions between ternary compound and FM, which coexist in the sample FE7 are also responsible for the maximum activity displayed. Beyond $x = 2.5$, the range of composition for the ternary compound formation is disturbed, possibly because the amount of bismuth available is less and hence only iron molybdate is formed. Pure $Fe_2(MoO_4)_3$ is known to be less effective for selective oxidation of olefins. Hence, the observed decrease in activity and selectivity for samples FE8 to FE11 could be attributed to the disappearance of ternary compound, the formation of ferric molybdate in increasing amounts, and the decrease in the surface concentrations of Bi, Mo, and Bi/Mo atomic ratio.

2.1 Studies on used catalysts. In order to elucidate the status of iron during reaction, used catalysts have been examined by IR spectroscopy and the degrees of reduction have been determined (Table 2). The IR spectra are presented in Fig. 7. It is seen that for used samples FE1, FE3, and FE5 all band positions are intact as in respective

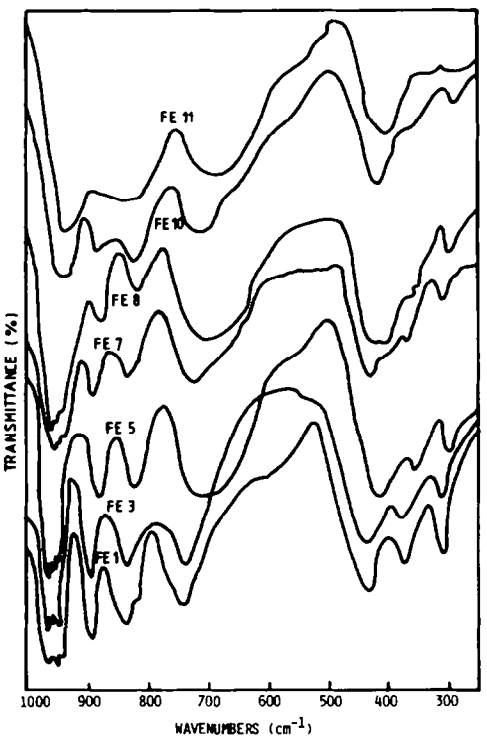

FIG. 7. Infrared spectra of used catalysts.

fresh catalysts indicating that under reaction conditions they are structurally stable and have undergone only surface reaction. This is also supported by the reduction number values. It seems that iron, through ternary compound formation ensures structural stability. Daniel and Keulks (*8*) have shown that the ternary compound is stable even under severe conditions of reduction. The spectrum of used FE7 indicates broadening of the band around 740 cm^{-1}, due to the formation of $FeMoO_4$. Spectra of samples FE8, FE10, and FE11 exhibit a broad band around 700 cm^{-1} due to $FeMoO_4$ and the intensities of the other bands are also reduced considerably. The reduction number values also indicate a higher degree of reduction. The band at 740 cm^{-1} is completely absent indicating that the multicomponent molybdate structure is disturbed.

CONCLUSIONS

The role of iron in the system $Mg_{11-x}Fe_x BiMo_{12}O_n$ appears to be quite complex. Formation of ternary compound between Be–Fe–Mo and the consequent increase in surface concentration of Bi and Mo results in increasing activity up to $x = 2.5$, at which point maximum activity corresponding to maximum Bi/Mo atomic ratio on the surface is observed. Interfacial effects between the ternary compound and $Fe_2(MoO_4)_3$ could also contribute toward activity. Beyond $x = 2.5$ disappearance of ternary compound, formation of inactive ferric molybdate and changes in surface concentration of Bi and Mo result in decreased activity. Ternary compound also appears to impart structural stability to the system, as shown by the IR spectroscopic study of the used catalysts, wherein with samples $x > 2.5$ (i.e., no ternary compound) reduction is deeper and major structural changes occur.

ACKNOWLEDGMENTS

We are indebted to Mr. B. U. Vala and Mrs. B. B. Solanki, for their assistance in carrying out the experiments.

REFERENCES

1. (a) Idol, J. D., Jr., U.S. Pat. 2,904,580 (1959); (b) Netherlands Pat. 7,006,454, issued to Nippon Kayaku Kabashiki Kaisha; (c) Yamaguchi, G., and Takenaka, S., U.S. Pat. 3,454,630.
2. Grasselli, R. K., and Hardman, H. F., U.S. Pat. 3,642,930 (1972).
3. Grasselli, R. K., Suresh, D. D., and Hardman, H. F., U.S. Pat. 4,001,317 (1977); U.S. Pat. 4,167,494 (1979).
4. Yoshino, T., Saito, S., and Sobu Kawa, M., Japanese Pat. 71.03,438 (1971).
5. Keulks, G. W., Krenzke, L. D., and Nottermann, T., "Advances in Catalysis," Vol. 27, p. 209. Academic Press, New York, 1978.
6. Annenkova, I. B., Alkazov, T. G., and Belenku, M. S., *Kinet. Catal.* **10,** 1305 (1969).
7. Batist, Ph.A., Van de Moesdijk, C. G. M., Matsura, I., and Schuit, G. C. A., *J. Catal.* **20,** 40 (1971).
8. Daniel, C., ad Keulks, G. W., *J. Catal.* **29,** 475 (1973).
9. Nottermann, T., Keulks, G. W., Skliarov, A., Maximov, Y., Margolis, L. Y., and Krylov, O. V., *J. Catal.* **39,** 286 (1975).
10. LoJacono, M., Nottermann, T., and Keulks, G. W., *J. Catal.* **40,** 19 (1975).
11. Sleight, A. W., and Jeitschko, W., *Mater. Res. Bull.* **9,** (1974).
12. Jeitschko, W., Sleight, A. W., McClellan, W. R., and Weither, J. F., *Acta Crystallogr. Sect. B* **32,** 1163 (1976).
13. Sleight, A. W., and Linn, W. J., *J. Catal.* **41,** 134 (1976).
14. Wolfs, M. W. J., Ph.D. thesis. Technische Hoge School, Eindhoven 1974; Wolfs, M. W. J., and Matsural I., *J. Catal.* **37,** 174 (1975).
15. Van Oeffelen, P. A. G., Ph.D. thesis. Technische Hoge School, Eindhoven, 1978.
16. Batist, Ph.A., *Surf. Technol.* **9,** 443 (1979).
17. Prasada Rao, T. S. R., and Menon, P. G., *J. Catal.* **51,** 64 (1978).
18. Forzatti, P., Villa, P. L., Feriazzo, N., and Jones, D., *J. Catal.* **76,** 188 (1982).
19. Wolfs, M. W. J., and Batist, Ph.A., *J. Catal.* **32,** 25 (1974).
20. Carter, W. J., Schweitzer, G. K., and Carlson, T. A., *J. Electron Spectrosc. Relat. Phenom.* **5,** 827 (1974).
21. Schofield, J. H., Lawrence Livermore Laboratory Rep. UCLR-51326 (1973).
22. Oganowski, W., Hanuza, J., Jezowska, Jrzbiatowska, B., and Wrzyszez, J., *J. Catal.* **39,** 161 (1975).
23. Trifiro, F., Hoser, H., and Scarle, R. D., *J. Catal.* **25,** 12 (1974).
24. Belyaev, I. N., and Smolyaninov, N. P., *Russ. J. Inorg. Chem.* (*Engl. Transl.*) **7,** 579 (1962).

25. Menon P. G., and Prasada Rao, T. S. R., *Catal. Rev.-Sci. Eng.* **20**(1), 96 (1979).

26. Venyaminov, S. A., Pitaeva, A. N., Bannik, G. B., Plyasova, L. M., Maksimovskaya, R. I., and Kustova, G. N., *Kinet. Katal.* **18**, 456 (1977).

27. (a) Burrington, J. D., Kartisek, C. T., and Grasselli, R. K., *J. Catal.* **81**, 489 (1983); **69**, 495 (1981); **63**, 235 (1980); **59**, 79 (1979); (b) Grasselli, R. K., and Burrington, J. D., "Advances in Catalysis," Vol. 30, p. 133. Academic Press, New York, 1981: (c) Grasselli, R. K., Burrington, J. D., and Brazdil, J. F., *J. Chem. Soc., Faraday Discuss.* **72**, 203 (1982).

28. Brazdil, J. F., and Grasselli, R. K., *J. Catal.* **79**, 104 (1983).

29. Brazdil, J. F., Glaeser, L. C., and Grasselli, R. K., *J. Phys. Chem.* **87**, 5485 (1983).